J Solid State Electrochem (2005) 9: 132–137
DOI 10.1007/s10008-004-0563-4

ORIGINAL PAPER

S. Migge · G. Sandmann · D. Rahner · H. Dietz
W. Plieth

Studying lithium intercalation into graphite particles via in situ Raman spectroscopy and confocal microscopy

Received: 13 February 2003 / Accepted: 16 April 2004 / Published online: 11 August 2004

Abstract The electrochemical intercalation of lithium into single graphite particles was studied in situ using Raman microscopy combined with confocal microscopy. The degree of intercalation during cycling was obtained from changes in the Raman bands of carbon. Confocal microscopy was used to image the graphite electrode in order to monitor the intercalation into single graphite particles. An industrial button cell was modified such that Raman spectra and microscopic images of the back side of the negative electrode could be taken through a window in the cup of the cell. The liquid electrolyte consisted of a 1:1 mixture of ethylenecarbonate/dimethylcarbonate (EC/DMC) with 1 M $LiPF_6$. The spectroscopy and microscopy showed that lithium does not intercalate into the graphite in a homogeneous manner. Inhomogeneous lithium intercalation was even observed in single graphite particles.

Keywords Lithium batteries · Raman spectroscopy · Confocal microscopy · Intercalation · Carbon particles

Introduction

The main process that occurs in a rechargeable lithium ion battery is the intercalation of lithium ions into different host materials. Different forms of carbon with a graphite structure are used as materials for the negative electrode. Of special interest are synthetic high temperature graphite, carbon fibers, and spherical mesocarbon microbeads [1, 2, 3]. One problem with these materials is the loss of charge capacity during the first charging process. A continuous but much smaller loss is observed in the following cycles. The origin of these losses is the formation of a surface layer at the carbon particle/electrolyte interface . In the first cycle a protective film is formed which allows the transfer of lithium ions but not the transfer of electrons. This layer is described as the "solid electrolyte interface" (SEI) [4, 5].

The intercalation of lithium ions into the carbon particle bulk is the real energy storage process. This process has been studied by many methods and techniques, including electrochemical methods as well as methods that provide local imaging. Despite these efforts, the local distribution of lithium across the surface of the graphite or carbon particles, and local variations in the degree of intercalation under in situ conditions in a working lithium battery are not yet known in detail.

Raman spectroscopy is a suitable method for studying the intercalation. When we began our research project (as work associated with the PhD of S. Migge [6]) and presented our first paper [7], we only found a few papers in the literature that dealt with the same subject [8, 9, 10]. However, since then, more applications of Raman microscopy to lithium graphite intercalation have been published [11, 12, 13]. While based on similar concepts, the results of these recent papers are valuable additions to our own results.

The graphite crystallizes in a hexagonal structure with the space group D^4_{6h}. Single crystal graphite has two doubly degenerate Raman active vibrational modes at 42 cm^{-1} (E_{2g1}) and at 1580 cm^{-1} (E_{2g2}) [14]. The mode at 1580 cm^{-1} is easily measurable and shows characteristic shifts and changes with increasing intercalation, and the formation of different intercalation stages of a formal Li:C ratio of LiC_{27}, LiC_{12} and LiC_6, as observed in experiments with highly ordered pyrolytic graphite (HOPG) [15]. Spectra of synthetic graphite do not differ from spectra of HOPG due to the identical processes that occur during intercalation.

In the present paper, results obtained from using Raman spectroscopy and confocal microscopy on a working graphite electrode will be described. The measurements were carried out with a typical industrial

S. Migge · G. Sandmann · D. Rahner · H. Dietz · W. Plieth (✉)
Institute of Physical Chemistry and Electrochemistry,
Technische Universität Dresden,
01062 Dresden, Germany
E-mail: waldfried.plieth@chemie.tu-dresden.de

button cell. The local variation in the degree of intercalation could be observed through a window in the cup of the cell.

In a practical cell there is a dense package of graphite, separator and positive electrode. It is impossible to investigate the graphite-separator interface. Normally, the intercalation process is assumed to be homogeneous. This means that the intercalating lithium ions will move inside the graphite material from the back. This is the place where optical measurements can easily be performed under practical conditions; where the intercalation process can be observed without being distorted by the closely packed separator. A further aim was to investigate the dependence of local variations in the degree of intercalation on the current density.

Experimental

Sample preparation

The active mass of the negative electrode was synthetic graphite LF-18D with an average particle diameter of 22 μm (Chuetsu Graphite Works Co.). The graphite was added to a solution of polyvinylidenefluoride (Solev 1010, Solvay SA) in *N*-methyl-2-pyrrolidone (Selectipur, Merck AG). The mixture (held oxygen free) was heavily stirred to get a homogeneous particle distribution. The suspension was applied to copper mesh (thickness 0.03 mm, Cu 10–118met, Exmet Corp.) with an applicator. The *N*-methyl-2-pyrrolidone was removed in two steps: at 100 °C under normal pressure for 10 min, and under vacuum at 85 °C for 1 h.

The electrolyte was ethylene carbonate (EC)/dimethylcarbonate (DMF) in the ratio 1:1 with 1 M $LiPF_6$. A commercially available mixture was used (LP30 Selectipur Merck AG). The water content was determined by coulometry (Metrohm 684 FK) and was less than 20 ppm. A microporous propylene film (Celgard 4518, Hoechst Celanese Corp.) was used as separator. The counter electrode was made of metallic lithium (99.99%, Aldrich).

Working cell

An industrial button cell (type 2016) fitted with an optical window was used for the investigations. A hole of 2 mm was drilled into the cell cup and a 1 mm thick glass plate was glued onto the cup (air and electrolyte proof). The principal components of the cell are shown in Fig. 1.

The cell was mounted in a glove box in argon atmosphere. The cup and the housing were pressed together with a force of 15 N. The cell contained 200 μl of electrolyte, bound preferentially in the porous graphite electrode and in the separator. Any influences from remaining moisture were minimized under these conditions.

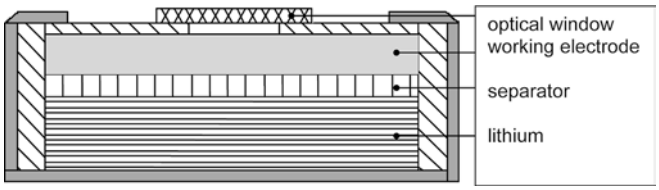

Fig. 1 Principal components of the working cell (Button cell, type 2016): cell housing consisting of steel, lithium counter electrode, separator, graphite working electrode, cell cup with through hole and window

Electrochemistry and Raman microscopy

The working electrode was placed on the scan table of a Raman microscope (Renishaw 2000). A He-Ne laser emitting light at 632 nm with a maximal power of 20 mW was used for illumination. The Leitz microscope was fitted with an ultra long distance objective (Olympus IC 80) for the Raman measurements. Spectra were obtained by adding 4×15 s spectra. The intensity was normalized. The microscope was also used for computer-aided imaging.A potentiostat/galvanostat (E&G, model 263) was used to electrochemically cycle the working cell. During the Raman measurements, the cycling was adapted to the registration time of the Raman microscope.

Results and discussion

Electrochemical behavior

Typical electrochemical behavior of the system is shown in the cyclovoltammogram in Fig. 2. In the first cycle, the typical peak from the formation of the solid electrolyte interface (SEI) is shown in the potential range 1.00–0.5 V. After charging (up to 0 V), the lithium deintercalates at about 0.2 V.

The SEI is formed in the first cycle (Fig. 3). This layer formation consumes the so-called ''irreversible charge capacity''.

The working electrode contained 5.7 mg graphite per cm^2. The cycling behavior corresponds to that reported in the literature for synthetic high temperature graphite [16, 17]. The irreversible capacity loss for the build-up of the solid electrolyte interface was 49 mAh/g. The reversible capacity of the first cycle was 327 mAh/g, 88% of the theoretical value. The efficiency was mainly dependent on the applied current density: the slower the intercalation, the higher the reversible capacity. The limiting current density for the working cell used was 0.12 mA/cm^2. Below this current density the change in the capacity was negligible. The applied current density for the Raman measurements was slightly higher (0.2 mA/cm^2), because at this current density the characteristic features of the intercalation process were most pronounced and could be followed on a practicable timescale.

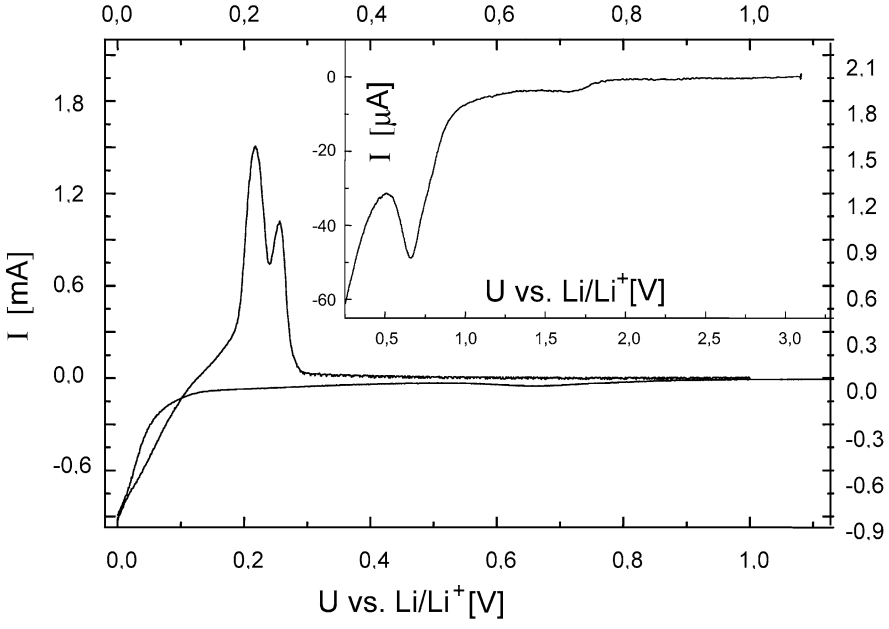

Fig. 2 Cyclic voltammogram of the first cycle of LF-18D with binder 10% Solev 1010 in electrolyte LP30, $v = 30$ µV/s. Insert: enlarged area of formation of the solid electrolyte interface. The counter electrode was metallic lithium

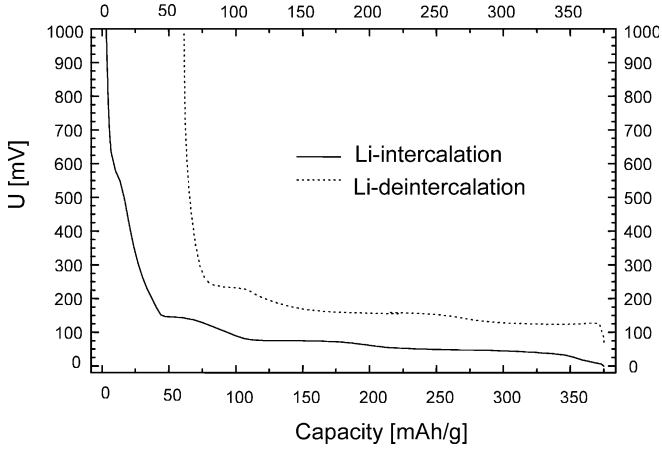

Fig. 3 Charging/decharging diagram of the first cycle of the working cell filled with LF-18D with 10% Solev 1010 in EC/DMC and 1 M $LiPF_6$. The counter electrode was metallic lithium

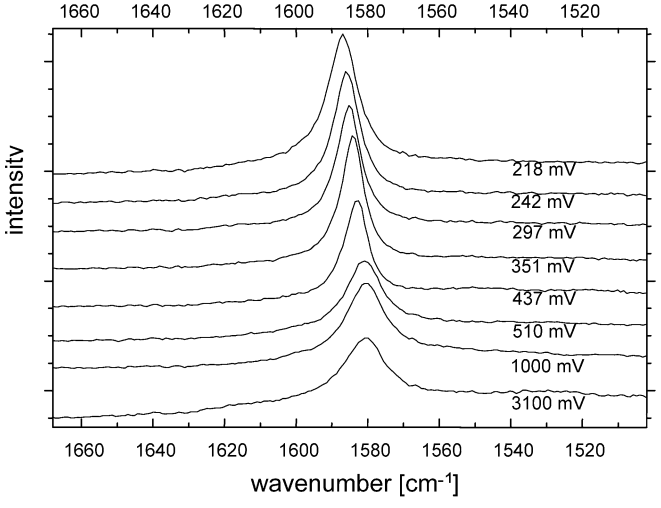

Fig. 4 In situ Raman spectra of graphite LF-18D for the first steps of intercalation (3.1 V–0.218 V)

The Raman spectra in the first part of the intercalation process (charging) are shown in Fig. 4 (3100 mV–218 mV).

Starting at the equilibrium potential (3100 mV), the Raman band at 1580 cm^{-1} does not change until the potential of 0.7 V is reached. The formation of the solid electrolyte interface at 0.7 V is not seen in the Raman spectrum. The intercalation of lithium into the graphite lattice starts at 0.5 V. The distance between adjacent graphite layers is increased by the intercalation but the lattice structure does not change. Under the influence of the lithium atoms, the wavenumbers are shifted to higher values. The maximum shift is 7 cm^{-1}. In the beginning, the intercalation occurs in statistical manner. As the degree of intercalation increases, a potential is reached at which the LiC_{27} phase is formed. In this structure two different types of graphite layers exist, one type not in direct contact with the lithium intercalation layer, the other one containing carbon atoms that are in contact with the intercalated ions. The result is the splitting of the E_{2g} band into two bands: one at 1575 cm^{-1} and one at 1600 cm^{-1}. Such a splitting has been reported in the literature [18] and is shown in Fig. 5.

The splitting is first seen as a broadening of the E_{2g} band, followed by the development of the double band. With increasing intercalation the band splitting slightly increases.

Figure 6 shows the spectra from 0.094 to 0.010 V, the endpoint of intercalation. In this region, the LiC_{12} structure is formed, and the double band disappears.

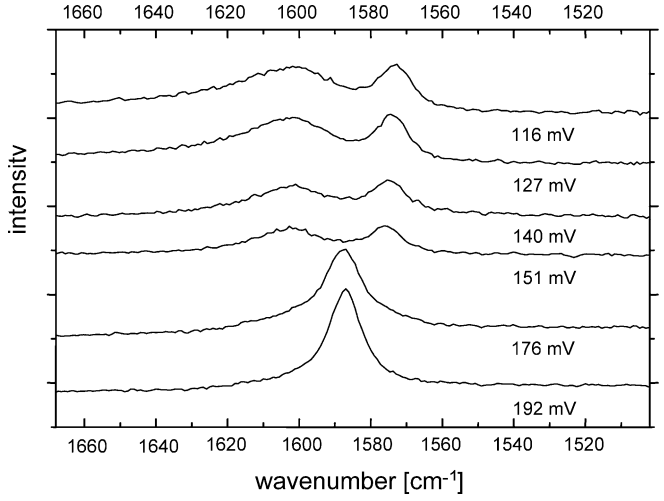

Fig. 5 In situ Raman spectra of graphite LF-18D from 0.192 V to 0.116 V, showing the splitting of the E_{2g} band

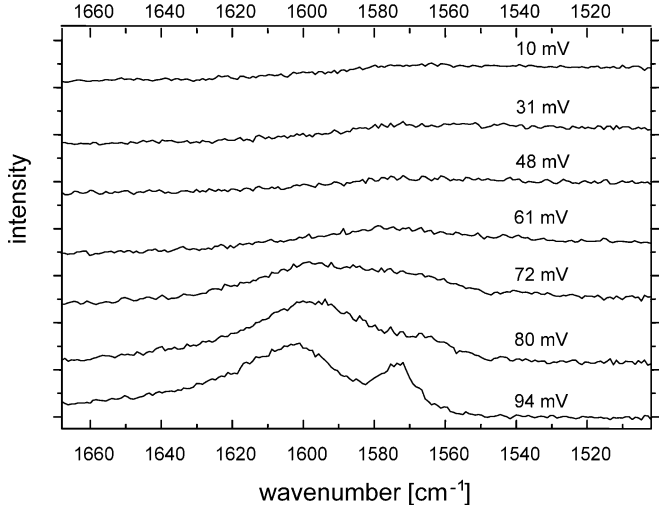

Fig. 6 In situ Raman spectra of graphite LF-18D from 0.094 V to 0.010 V, showing the disappearance of the double band

All graphite layers are of the same structure, always having one intercalation layer as a neighboring layer. But the band broadens while the band intensity decreases until the band has disappeared. Consequently, the LiC_6 structure does not show the E_{2g} band. This is explained by the high electric conductivity of the fully occupied lithium intercalation layers, causing strong absorption and reduced thickness of the surface film, scattering the Raman light [19]. Therefore, investigation of lithium ion intercalation into graphite with Raman spectroscopy is limited to low or medium degrees of intercalation. With increasing intercalation the signal-to-noise ratio decreases until the signal disappears in the noise. But clear assignment of the spectra to different intercalation structures is possible in the region where spectra are observed. The shifted band at around 1575 cm^{-1} belongs to statistical intercalation, the double band to the LiC_{27} structure, and the broad and noisy band of 1560–1600 cm^{-1} belongs to the formation of LiC_{12}.

The described processes are reversible, with a hysteresis of approximately 100 mV. This is shown in Fig. 7, where the potential is varied from 120 to 1000 mV. The spectra appear in reverse order. First the 1600 cm^{-1} band appears (162 mV), it is split into two bands. The double band moves over (at potentials above 244 mV) into the frequency-shifted E_{2g} single band (shown at 520 mV). Finally, even the shift has disappeared and the band of the non-intercalated graphite at 1570 cm^{-1} is obtained.

Raman spectra on single particles

The Raman spectra shown so far were obtained from a larger surface area. In Fig. 8 two microscopic images of single graphite LF-18D-particles on the back side of the graphite electrode are shown. The characteristic features of the images are the different colors of the surfaces of the graphite particles. It will be shown that these colors represent different degrees of intercalation.

Figure 9 shows Raman spectra measured at the different local positions marked in Fig. 8. Points A and B show spectra identified as different degrees of intercalation of the LiC_{12} structure. At point C, the graphite is still in the LiC_{27} structure. The spectra for D and E indicate that these are regions of the particle where the intercalation has reached the intercalation limit LiC_6.

The Raman spectra not only show the degree of intercalation at the particle's surface, but also in a region below the surface of the particle. The penetration depth is of the order of 100 nm at wavelengths around 500 nm [20]. It is even larger at a wavelength of 632 nm. This

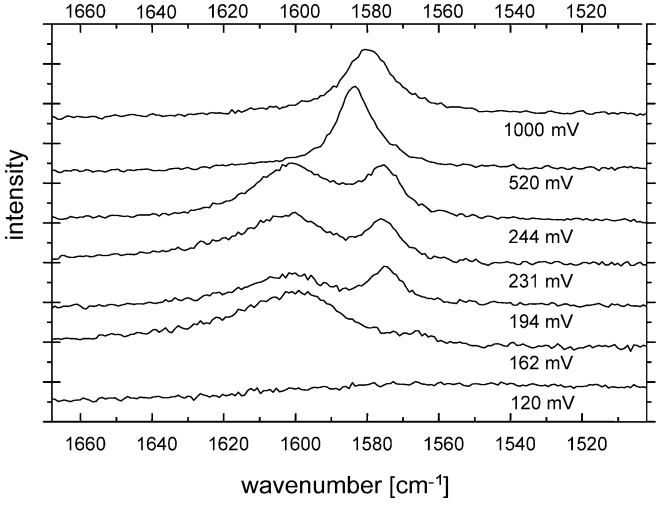

Fig. 7 Illustration of the reversibility of the intercalation process. When decharging the graphite electrode (deintercalation), the Raman bands from 0.120 V to 1.000 V vary in the reverse manner to those in Figs. 4–6

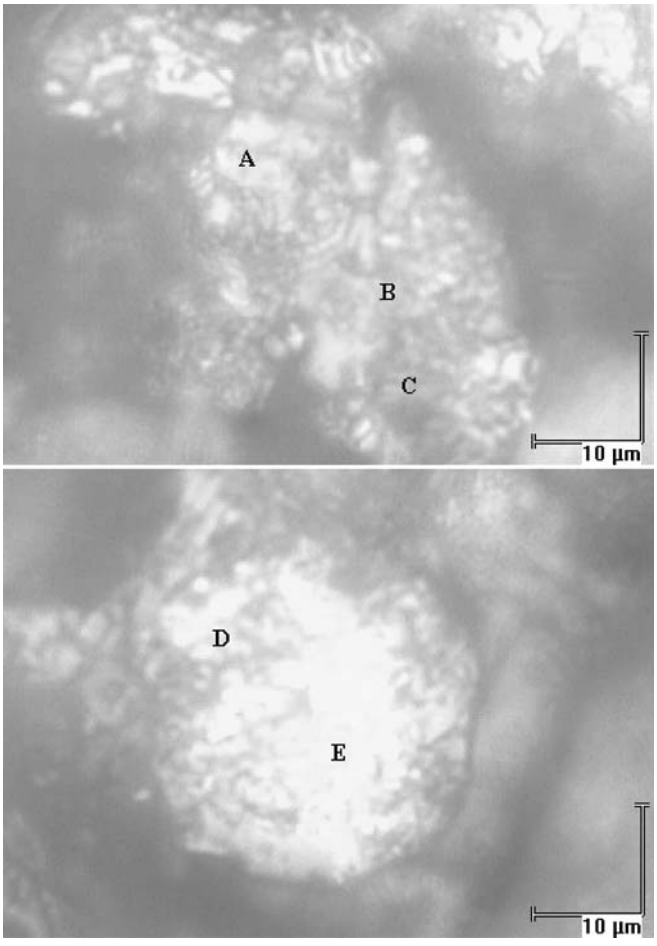

Fig. 8 Microscopic images of two graphite particles (LF-18D) on the back side of the graphite electrode. The different colors represent regions with different degrees of intercalation (over one cycle). The letters A–E indicate where local Raman spectra were measured; these Raman spectra are shown in Fig. 9

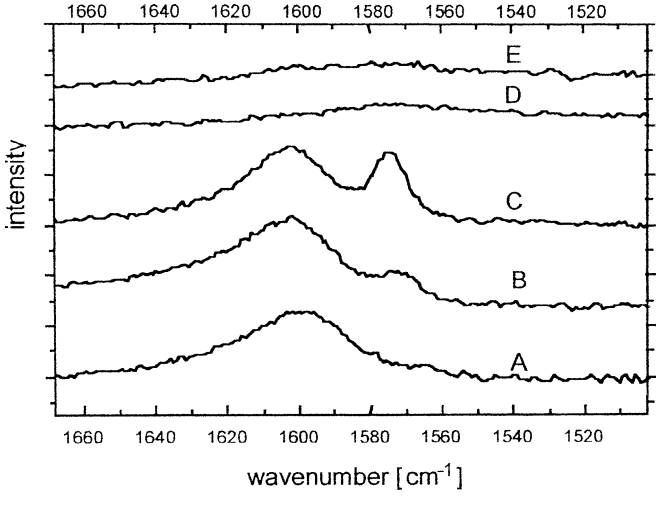

Fig. 9 Raman spectra measured at different surface points on the graphite particle, as shown in Fig. 8 (the letters A–E correspond to the positions in Fig. 8)

shows that Raman spectroscopy and microscopy, while preferentially a surface sensitive method, represents not only the status of the surface of a particle but also that of bulk areas below the surface of the sample.

By comparing Figs. 8 and 9, one can see that the degree of intercalation is qualitatively obtained by the color of the graphite particle surface. Up to the lowest defined intercalation structure LiC_{27}, the color is gray to blue, the intermediate structure LiC_{12} is red, while the highest degree of intercalation (LiC_6) has a characteristic gold-yellow color.

The degree of intercalation shows significant differences from particle to particle. The intercalation starts at the parts of the particle pointing towards the electrolyte reservoir. While the majority of the particles of the electrode are still dark, some particles already show a change in color towards red (LiC_{12}). This means that the lithium ions are transported by diffusion through the electrolyte in the graphite electrode. The results emphasize the importance of the electrolyte balance in the graphite electrode for the performance of the battery.

The different degrees of intercalation for different particles, and even on the surface of a specific particle, shows a further feature of the electrode. The result should be a variation in the potential within the electrode, like in a corrosion process, with different materials. The measured potential is, however, an average value; various surface regions can have potentials differing from the average value, and they will cause a "contact corrosion" leveling of the lithium concentration in the carbon material over time.

Finally, some general observations about the dependence of the intercalation process on the surface structure can be made from Fig. 8. There is no preferential surface structure for preferential intercalation. The intercalation starts at various interfaces. Maybe crystallographic misfits, dislocations, steps, and so on, are the reason for this indifferent behavior. Sometimes a surface area shows a very fast intercalation, which can be explained by a very high density of surface defects. Opposite results were reported for HOPG [21].

The intercalation behavior was strongly dependent on the current density. As current density was increased, a fast saturation of the surface was observed, accompanied by a fast potential delay. Under these conditions a low capacity was measured due to the low degree of intercalation in the bulk of the graphite particles.

Conclusions

Raman spectroscopy combined with confocal microscopy is a powerful tool that can be used to study the intercalation of lithium ions into graphite. With these methods, the intercalation on a graphite electrode can be observed on single graphite particles. The results show the dependence of the degree of lithium intercalation on various parameters of working batteries, like current

density, electrolyte, and temperature. This intercalation is not a homogeneous process; it varies with the crystallographic and local conditions.

In the future, this method could become a useful tool for the screening and optimization of different graphite materials for advanced battery performance. So far only the graphite electrode has been investigated. The steadily increasing sensitivity of modern Raman micro-spectrometers might allow us to answer further questions about the lithium ion battery system.

Acknowledgements We thank the Saechsische Ministerium fuer Wirtschaft und Arbeit for supporting this research. General support of this research by the Fonds der Chemischen Industrie is also acknowledged.

References

1. Aurbach D, Markovsky B, Shechter A, Ein-Eli Y (1996) J Electrochem Soc 143:3809
2. Tokumitsu K, Mabuchi A, Fujimoto H, Kasuh T (1996) Eighth Int Meeting on Lithium Batteries, Nagoya, Japan, 16–21 June 1996, Extended Abstracts, p 212
3. Yun M, Moon S, Doh C, Lee K (1995) Synthetic Met 71:1761
4. Besenhard JO, Winter M, Lutter W (1995) J Power Sources 54:28
5. Ogumi Z, Inaba M (1998) Bull Chem Soc Jpn 71:521.
6. Migge S (1999) Dissertation. Fakultaet fuer Mathematik und Naturwissenschaften, Technische Universitaet Dresden, Germany
7. Migge S, Sandmann G, Plieth W (2000) Annual Meeting of the Deutsche Bunsengesellschaft fuer Physikalische Chemie, ''Electrochemical energy storage and transformation'', Wuerzburg, Germany
8. Irish DE, Deng Z, Odziemkowski M (1995) J Power Sources 54:28
9. Cazzanelli E, Mariotto G, Decker F, Rosolen JM (1996) J Appl Phys 80:2442
10. Inaba M, Yoshida H, Ogumi Z (1996) J Electrochem Soc 143:2572
11. Rey I, Lasségues JC, Baudry P, Majestre H (1998) Electrochim Acta 43:1539
12. Panitz JC, Novák P, Haas G (1999) Appl Spectrosc 53:1188
13. Panitz JC, Joho F, Novák P (2001) Appl Spectrosc 55:1131
14. Nemanich RJ, Lucovsky G, Solin SA (1977) Solid State Commun 23:117
15. Inaba M, Yoshida H, Ogumi Z, Abe T, Mizutani Y, Asano M (1995) J Electrochem Soc 142:20
16. Tarascon JM, Guyomard D (1993) Electrochim Acta 38:1221
17. Bittihn R, Herr R, Hoge D (1993) J Power Sources 43:223
18. Sokin SA (1990) In: Zabel IH, Solin SA (eds) Graphite intercalation compounds. Springer, Berlin Heidelberg New York, p 181
19. Dresselhaus MS, Dresselhaus G (1981) Adv Phys 30:139
20. Huang W, Frech R (1998) J Electrochem Soc 145:765
21. Tran TD, Kinoshita K (1995) J Electroanal Chem 386:221